Environmental Earth Sciences (2019) 78:95
https://doi.org/10.1007/s12665-019-8049-y

ORIGINAL ARTICLE

Identifying natural and anthropogenic variability of uranium at the well scale, Homestake Superfund site, near Milan, New Mexico, USA

Philip T. Harte[1] · Johanna M. Blake[2] · Jonathan Thomas[3] · Kent Becher[3]

Received: 8 September 2018 / Accepted: 7 January 2019

Abstract
The San Mateo Creek Basin in New Mexico, USA is located within the Grants Mineral Belt-an area with numerous uranium (U) ore deposits, mines, and milling operations. Six monitoring wells set in an alluvial aquifer near the Homestake Mining Co. Superfund site in the lower San Mateo Creek Basin were logged with a suite of borehole geophysical tools including spectral gamma-ray (SGR), vertically profiled with passive samplers for U and selenium (Se) concentrations, and purged sampled for same constituents. The integrated approach allowed for an assessment on the role of heterogeneity (both physical and chemical) in determining U concentrations in groundwater. Uranium, as measured with SGR logging, is ubiquitous in the alluvial aquifer and the underlying Chinle Group. Aqueous U concentrations appear to be inversely related to thorium (Th) concentrations, as measured by the SGR log, indicating the possibility that U is bound in or adsorbed to clays in the aquifer. The stratigraphy of the alluvium likely plays a role in elevated concentrations of aqueous U. Interbedded clay and sand layers allow for the mobilization of U in oxic sandy layers from U adsorbed in sediments in reduced clay layers. The stratigraphy also plays a role in the degree of mixing of groundwater in the formation and well. Mixing can obscure the ability to identify U sources. Mixing is exacerbated by the relatively long screens (> 20 ft long or > 6.1 m) of the monitoring wells.

Keywords Spectral gamma-ray · Passive samplers · Micropurge · Uranium · Selenium

Introduction

The natural physical and chemical heterogeneity of a groundwater-flow system can complicate the identification of ambient concentrations of uranium (U). Further, the use of monitoring wells with long screens (> 20 ft or > 6.1 m) for sampling can cause mixing of groundwater from different hydrogeologic units and formations, each with potentially unique U concentrations and water types.

While heterogeneity is a factor, variable sources of U, such as natural and anthropogenic (enrichments caused by mining or other activities), are also problematic in distinguishing natural background concentrations of U. Activities such as mining and milling can cause enrichment of U as evidenced by elevated aqueous U concentrations in groundwater, association with co-contaminants such as molybdenum (Mo), selenium (Se), and alterations to the common U isotopes of ^{234}U, ^{235}U, and ^{238}U (Zielinski et al. 1997). When there are multiple mining and milling sources, distinguishing between these anthropogenically enriched sources is further complicated.

Elevated concentrations of U and co-occurring constituents, such as Se and Mo, in groundwater have been detected at and surrounding the Homestake Mining Co. Superfund site (Site) near the village of Milan (hereafter referred to as Milan), New Mexico (Fig. 1a) (Hydro-Engineering 2001). The groundwater may be affected by undisturbed ore deposits (natural sources) and mining or milling activities

Electronic supplementary material The online version of this article (https://doi.org/10.1007/s12665-019-8049-y) contains supplementary material, which is available to authorized users.

✉ Philip T. Harte
ptharte@usgs.gov

[1] U.S. Geological Survey, 720 Gracern Rd, Columbia, SC 29210, USA

[2] U.S. Geological Survey, 6700 Edith Blvd. NE, Albuquerque, NM 87113, USA

[3] U.S. Geological Survey, 501 W. Felix Street Bldg 24, Fort Worth, TX 76133, USA

Published online: 01 February 2019

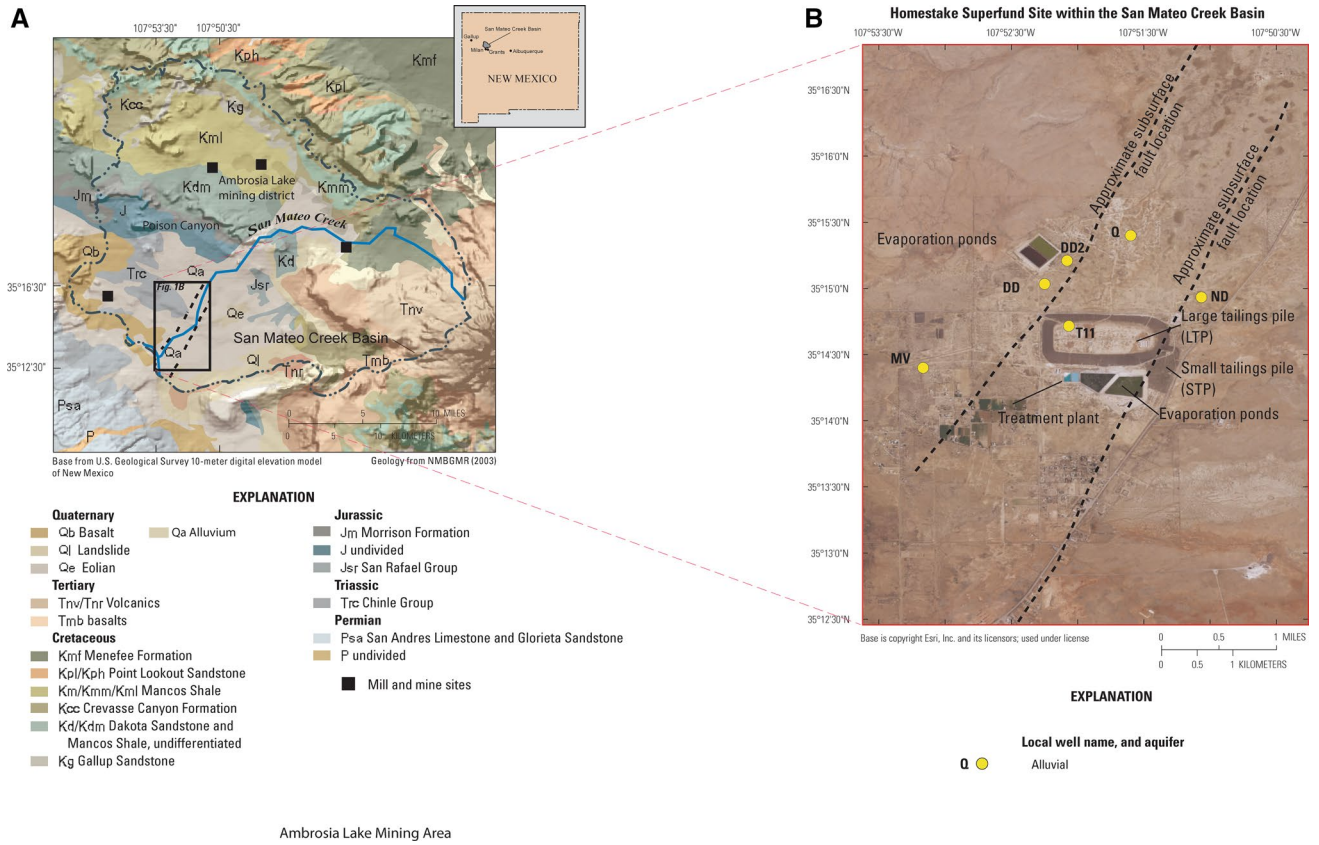

Fig. 1 The location of study area showing the San Mateo Creek Basin, and logged and sampled wells, Homestake Superfund site, near Milan, New Mexico, USA (The Grants Mineral Belt covers much of **a**)

(anthropogenic sources). Locally, two tailings piles, large (LTP) and small (Fig. 1b), located on the Site, likely affect the water quality in adjacent aquifers. Regionally, dewatering of uranium mines in the upper San Mateo Creek Basin and the Ambrosia Lake mining district (Fig. 1a), located north of the site, have led to the contamination of downstream sediments from stream transport, and downgradient groundwater in the alluvial and underlying rock aquifers (via faults) (Gallaher and Goad 1981; Schoeppner 2008) because mine waters were discharged into natural waterways without treatment (Langman et al. 2012). Uranium and Mo are considered the most mobile elements from U mill sites and Se is also associated with U ore (Morrison and Spangler 1992). Selenium concentrations related to the Poison Canyon area, located upgradient (northwest) of the Site, are generally high (Gallaher and Cary 1986) (Fig. 1a). To the northeast of the Site, solid U concentrations from surficial material are low and indicate a naturally low U source rock (NURE 2017).

This paper focuses on the role that physical and chemical heterogeneity plays in the variability of U concentrations in groundwater of the alluvial aquifer at the Site within the framework of distinguishing natural and anthropogenic sources of U. This work is part of a larger study to differentiate chemical signatures in the water with one or more U sources using geochemical and isotopic analyses (Harte et al. 2018b).

Site description

The Site received processed raw U ore material from external sites starting in 1958; from 1958 to 1990 milling activities continued. Other contaminants of concern associated with U include thorium-230, radium-226, radium-228, Se, Mo, sulfate, and dissolved solids. The LTP was constructed starting in the early 1960s without a liner, and processed materials, including wastewater as a transporting device, were deposited onto the LTP. Waste water infiltrated into a surficial alluvial aquifer from both the LTP and a small tailings pile (STP) [U.S. Environmental Protection Agency (EPA) 2010] (Fig. 1b). Beginning in 1977 and until the present, various levels of remedial activities have been initiated to contain the spread of a U plume emanating from the site. Activities have included the flushing of the tailings from 2000 to 2015 with uncontaminated groundwater from a lower aquifer. Private wells in the residential subdivisions south of the Site have elevated levels of contaminants (EPA

2011). All residences have been connected to an alternate water source from Milan (EPA 2011).

The Site is underlain by alluvium with a saturated thickness that thins from west (50 ft or 15.2 m) to east (20 ft or 6.1 m) (Hydro-Engineering 2001). Underlying the alluvium are the Triassic-age Chinle Group and the Permian-age San Andres Limestone and Glorieta Sandstone. The underlying more permeable layers of the rocks consist of sandstone, limestone, and siltstone. The Chinle Group comprises three aquifers (upper, middle, and lower) separated by shale. Some or all of the underlying rock aquifers (the three Chinle aquifers in particular) subcrop in various locations in the San Mateo Creek Basin. The dip of the Chinle Group, San Andreas Limestone, and Glorieta Sandstone is approximately to the north, which is counter to regional flow in the alluvial aquifer, which is generally from northeast to southwest (Hydro-Engineering 2001).

Groundwater in the alluvial aquifer recharges the Chinle aquifers at subcrop locations. The rate of recharge from the alluvial aquifer to the Chinle aquifers is dependent on changes in the saturated thickness of the alluvial aquifer as waters from upgradient mining legacy locations in the San Mateo Creek Basin are transported downgradient. The lower rock aquifers are intersected by a series of faults. One set of faults trends from southwest to northeast and bounds the area of the LTP (Fig. 1b). The underlying rock aquifers are uplifted to the west of the LTP.

The Site remediation standard for U is 160 micrograms per liter (µg/L) and for Se it is 320 µg/L for the alluvial aquifer, which is based on concentrations of contaminants of concern of well water from the alluvial groundwater interpreted as being upgradient from the Site (EPA 2011). Due to recharge of groundwater from the alluvial aquifer to the Chinle aquifers, groundwater standards are being applied to the Chinle aquifers in the affected area (called mixing zone). The remediation standards do not meet Federal drinking water standards for U (Maximum Contaminant Level (MCL) of 30 µg/L; EPA 2016) and Se (MCL of 50 µg/L; EPA 2016), which is partly due to pervasive mining activities in the upper San Mateo Creek Basin and the potential for regional contamination to impact local water quality.

Historical U concentrations in groundwater

Historical regional data for the Grants Mineral Belt area show mean background concentrations of 23 µg/L for U in groundwater (Kaufman et al. 1976). Uranium concentrations less than 100 µg/L for the middle to lower San Mateo Creek Basin were considered unaffected by mining activities (Gallaher and Cary 1986). In more recent work, regional U concentrations in groundwater from the San Mateo Creek Basin ranging from < 10 to 500 µg/L have been measured (New Mexico Environment Department (NMED) 2008; 2012). A study by EPA (2018) found U concentrations of alluvial groundwater in the San Mateo Creek Basin upgradient from the Site ranging from 2 to 300 µg/L.

Wells located far upgradient (> 0.8 km; > 0.5 mi) from the LTP (to the north) are hypothesized to be affected by regional mining/milling contamination from the upper San Mateo Creek Basin as shown by increases in contaminants associated with regional mine and milling wastes (Homestake Mining Co. 2015). Closer to the Site, proximal wells located just north of the Site (interpreted as being upgradient from the LTP; Homestake Mining Co. 2015) could be affected by local mounding and radial outflow from LTP wastewaters. Because of local mounding at the LTP, proximal wells to the north could be downgradient from the LTP despite the prevailing regional flow direction of northeast to southwest. Several of the proximal wells show a wide range of U concentrations (from 20 to 230 µg/L) based on 1995–2004 data as reported by Homestake Mining Co. (2015) and Hydro-Engineering LLC (2001).

Geochemistry of U and Se occurrence

At the concentrations of dissolved U in most natural waters, U solubility is most likely limited by sorptive processes and not by U mineral saturation (Langmuir 1978). Uranium mobility is affected by redox, pH, and aqueous complexes. The insoluble form U(IV) is predominant in U ore (Brookins 1977; Hall et al. 2017), but once exposed to the surface through mining or milling, the oxidation state becomes U(VI) (Basu et al. 2015; Van Berk and Fu 2017; Dong and Brooks 2006; Alam and Cheng 2014; Klaja and Dudek 2016), which is much more mobile in water.

Uranium roll-front type deposits have been noted in the Poison Canyon area upgradient (northwest) from the Site with the occurrence of U ore being associated, stratigraphically, near the location between coarse-grained units with oxygenated groundwater and fine-grained interbeds with reduced groundwater (Turner-Peterson and Fishman 1986). Roll-front deposits that form in oxidized to reduced zones have a preferential sequence of deposition from (1) Se with hematite, (2) vanadiferous clay plus U silicate or oxide plus pyrite or marcasite, and (3) pyrite or marcasite plus jordisite (Brookins 1977). Oxidizing agents can remove pyrite and carboniferous material. Some studies have shown an association of U with carbon-rich environments, whereas others have shown no association (Fabricius et al. 2003).

Selenium has been associated with salts and irrigation water in arid environments such as New Mexico. Selenium occurs in four oxidation states as selenate (SeO_4^{2-}, 6+ oxidation state), selenite (SeO_3^{2-}, 4+ oxidation state), elemental selenium (Se^0, neutral), and selenide (Se^{2-}, 2− oxidation state) (McNeal and Balistrieri 1989). Selenate and selenide generally are soluble in water, whereas elemental Se and

most forms of selenide are insoluble (Bailey et al. 2012; Masscheleyn et al. 1990; Gates et al. 2009; Mast et al. 2014). Selenate is highly mobile, especially under alkaline and oxidizing conditions (Naftz and Rice 1989), because its salts are highly soluble and it is weakly adsorbed to particles (McNeal and Balistrieri 1989). Selenite is stable in alkaline to mildly acidic conditions and is more readily immobilized by adsorption onto clay minerals, organic matter, and iron oxyhydroxides (McNeal and Balistrieri 1989; Balistrieri and Chao 1990; Boult et al. 1998). Microbial action can change the speciation of Se through changes in redox state or the formation of organic Se compounds (Wright 1999; Gates et al. 2009; Bailey et al. 2012; McNeal and Balistrieri 1989; Kulp and Pratt 2004; Dubrosvky et al. 1990).

Approach

Uranium variability at 6 monitoring wells (Fig. 1b) was assessed relative to the level of heterogeneity of the formation to gain insight into U occurrence from natural and anthropogenic sources. The 6 monitoring wells are located upgradient (to the north), proximal, and downgradient (to the south) from a local U source (Site). Well construction information for the 6 monitoring wells is included in supplemental information (s1). We examined the level of heterogeneity in alluvial stratigraphy with a standard suite of borehole geophysical logs including natural gamma-ray (NGR). Because NGR is a bulk signal and responds to K, Th, and U combined, we also utilized spectral gamma-ray (SGR) logging to help differentiate NGR responses (Keys 1990). In addition to NGR and SGR, the other borehole geophysical logging (electromagnetic (EM) induction, fluid conductivity and temperature logs, flowmeter) was used to identify the level of the physical and potential chemical heterogeneity of the alluvium, confirm well construction and condition (optical televiewer log), determine which hydrogeologic layers each well screen is open to, the degree of mixing external to the well in the formation (EM induction logs) and internal to the well (fluid conductivity and temperature logs), and to identify the lithology, mineralogy, and gamma emitting elements (NGR and SGR logs).

The synthesis of results from borehole logging can help discern the degree of heterogeneity and fluid mixing in wells. For example, the variability in the NGR log can identify interbedding and contrasting lithologic and mineralogic layering in the alluvium. Large differences between maximum and minimum measurements indicate large contrasts in bedding. The relation between K, U, and Th can be used for distinguishing the type of minerals, type of deposits, and the presence of organic matter. Organic matter content in rocks can be a factor in binding U in reducing environments. Thorium is an indicator of clay content, types of clay minerals, and heavy minerals in igneous rock (not applicable in the study area). Potassium (K) is an important component in shales and is an indicator of feldspars and micas; K generally occurs in oxidized form. The ratio of Th/K is important for distinguishing the type of clay minerals (Klaja and Dudek 2016).

Coupled with the logging, vertical strings of passive samplers were deployed along potential stratigraphic and other hydrochemical boundaries as identified from the borehole logging. The passive samplers were used to profile the well for aqueous U and Se concentrations under ambient conditions. In this way, the bulk signal (aquifer and water) from the borehole geophysical logs can be compared to the aqueous concentrations measured from water in the passive sampler.

We also determined U and Se concentrations in purge samples that represent water from different parts of the formation than the water from the passive samplers. The two purge sample methods included micropurge (small volume) and volumetric (large volume). A schematic identifying the potential differences in sample zones based on sample method is shown in Fig. 2. The micropurge sample method collected water from a small zone of the well and likely from a small zone of the formation (Fig. 2). In contrast, samples collected during volumetric pumping of a well,

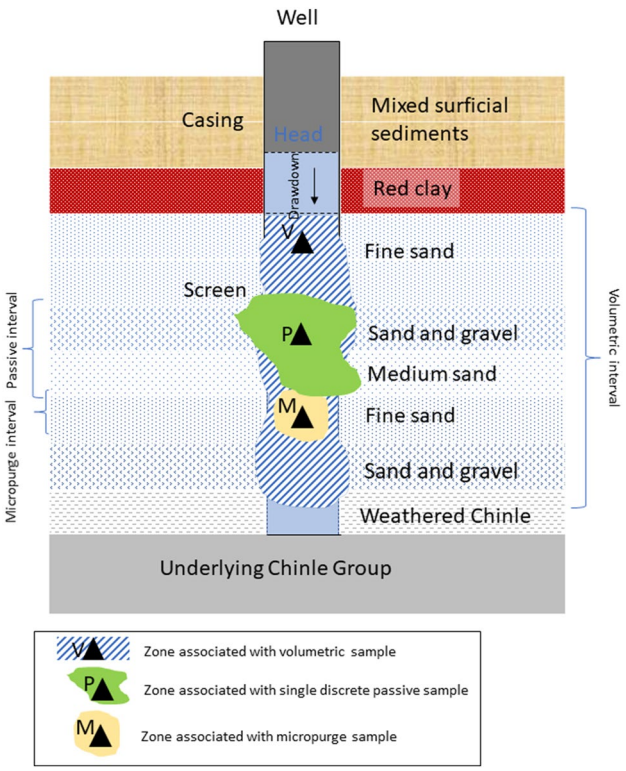

Fig. 2 A schematic of sample zones for the different sampling methods (This figure shows a conceptual view of a sampler zone associated with one single passive sampler. For a vertical profile of passive samplers, a larger vertical sample zone would result)

where large volumes of water are pumped, are intrinsically flow-weighted and preferentially collected water from the more permeable units. Volumetric samples likely collected water from a larger interval of the well and formation than the other methods (Fig. 2). For passive samples, the zone of sample is likely smaller than the volumetric sample but may be comparable to the micropurge sample (Fig. 2). The sample zone for the passive sampler is particularly dependent on the ambient flow patterns of the well (i.e., intraborehole flow).

Methods

Borehole geophysics

Conventional borehole geophysical logs were collected at the 6 monitoring wells (supplemental information s1) and included optical televiewer, caliper, NGR and SGR, fluid conductivity, fluid temperature, and EM induction logs. Three wells had vertical-differential flowmeter logs run under ambient and stressed (pumped) conditions. The geophysical data are available at https://doi.org/10.5066/F7CR5RJS (Harte et al. 2018b).

All borehole geophysical data were collected using a Century Geophysical Corporation system VI logging system or a Mount Sopris Instruments Matrix logging system. For this study, the Mount Sopris Instruments system was used to collect optical televiewer, fluid property, and SGR logs; all other logs were collected using the Century Geophysical Corporation system. Limitations, calibration procedures, and algorithms of the geophysical probes are available from the manufacturers (Century Geophysical Corporation 2017; Mount Sopris Instruments 2017).

All logs were collected according to the American Society of Testing and Materials (ASTM) borehole geophysical standard procedures (ASTM 2004, 2007, 2010). Geophysical logs were collected in digital format and were recorded in the proprietary format of the data acquisition equipment used to collect the logs. These proprietary data formats were converted to and stored as Log American Standard (LAS) Code for Information Interchange (ASCII) Standard (Canadian Well Logging Society 2013) for tabular data and presented as chart logs in a portable document format (PDF) file (Harte et al. 2018b). Only the NGR and SGR logs are described in detail here. Information on other logs (fluid, EM induction, and EM flowmeter) can be found in Keys (1990).

The NGR logs provide a record of gamma radiation measured in a borehole and are unaffected by well fluids. A scintillation detector is used in NGR tools to measure the natural gamma-ray emission from radioactive material in the formation. The primary emitters are potassium (^{40}K), ^{238}U, and thorium (^{232}Th). As each of these isotopes decay, the energy released contributes to the total NGR log. Typically, fine-grained sediments that contain abundant clay tend to be more radioactive than coarse-grained sediments, quartz sandstones, or carbonates (Keys 1990). The unit of measurement is API (American Petroleum Institute units).

The SGR logs were used to identify individual gamma emitters from the potassium (^{40}K), uranium (^{238}U) and thorium (^{232}Th) decay series encountered in the alluvium and underlying formations (Ehrenberg and Svånå 2001). The K isotope is directly detected by its gamma emission, whereas the U and Th emiters show up through the signatures of daughter products, and the SGR assumes radiometric equilibrium has been achieved before counts in the U and Th spectral windows can be quantitatively related to the presence of these elements. A Mount Sopris 2lsa-1000 large-crystal-spectral-gamma probe (https://mountsopris.com/items/2lsa-1000-large-crystal-spectral-gamma/) was used.

The SGR logs were collected in nonstationary (trolling) and stationary (parked) modes. Nonstationary mode (trolling) was carried out similar to other logs by moving the tool up or down at a fixed rate (3–10 ft/min or 0.9–3.3 m/min). There is some uncertainty about the reliability of SGR logs in trolling mode and for this reason we chose to look at bulk responses of the individual gamma emitters. We used the relative ranking of a well's summary statistics from trolling measurements to assess trends. Stationary mode was collected at 3–8 specific depths per well and measurements allowed to stack to collect a more statistically robust measurement that was then averaged and reported. The stacked measurements (from below the water table) are generally in agreement within one or two ranked positions with the trolling statistics for most wells meaning if the well fluid had a relatively high or low radioactive element concentration for the trolling statistics this was also the case for stacked measurements based on mean statistics.

Chemical profiling and groundwater sampling

Passive, micropurge, and volumetric groundwater samples were collected in July–October 2016 for this study (Fig. 2). All collected samples were kept on ice and submitted for laboratory analysis for U and Se, as described in the following section "Laboratory Analysis." Additional groundwater sampling details are provided in Harte et al. (2018a).

Passive samples were collected first in the sampling process. Nylon screen (NS) passive samplers were used to collect the passive samples and map the vertical variation in well chemistry (specifically U and Se). A maximum number of 11 NS passive samplers was deployed at well T11, and all wells had at least 7 samplers. The NS passive samplers (Vroblesky et al. 2002, 2003a, b) were deployed in 6 monitoring wells according to methods described by Harte et al.

(2018a). The NS mesh has a 125-micrometer opening and represents a quasi-filtered sample. However, because the NS mesh is coarser than a 0.45-micrometer filter commonly used to collect dissolved samples, the sample is designated as total (unfiltered).

The micropurge sample was collected second. The primary purpose of a micropurge sample was to allow a direct comparison to the results of the passive samplers, which serves as calibration of the passive sampler.

Volumetric samples were collected last. Volumetric samples were collected after removal of a quantified volume (three times the volume of water in the static water column of the well casing and screen prior to sample collection), to achieve a representative sample of groundwater (Harte et al. 2018a). During volumetric purging, concurrent monitoring measurements of field parameters were collected until the readings stabilized, which helped ensure the capture of formation water (USGS, variously dated; Harte et al. 2018a, b). The pump intake was set in the solid casing, just above the top of the screen. In the absence of water in the casing (called casing water), the pump intake was placed at the midpoint of the open interval.

Laboratory analysis

Groundwater samples for U and Se concentrations were analyzed by EPA method 6020A (inductively coupled plasma mass spectrometry (ICPMS)) at RTI labs, Livonia, MI. A subset of dissolved U samples was submitted to the EPA Region 6 lab for further analysis (ICPMS, EPA 200 series, method ILMO5.3; Martin 2003). A detailed report of laboratory concentrations and quality control and assurance is provided in Harte et al. (2018a).

Geophysical logging results

Both the NGR and EM induction logs for the six wells show variability with depth indicating various levels of heterogeneity as inferred from geophysical logs. Two wells (ND and DD) are highlighted to illustrate the type of heterogeneity encountered (Figs. 3, 4). Groundwater from wells ND and DD have relatively low and high historical U concentrations, respectively (Hydro-Engineering 2001).

At well ND, a brown sand layer [Fig. 3; depth of 35 ft or 10.7 m below land surface (bls)] is associated with an

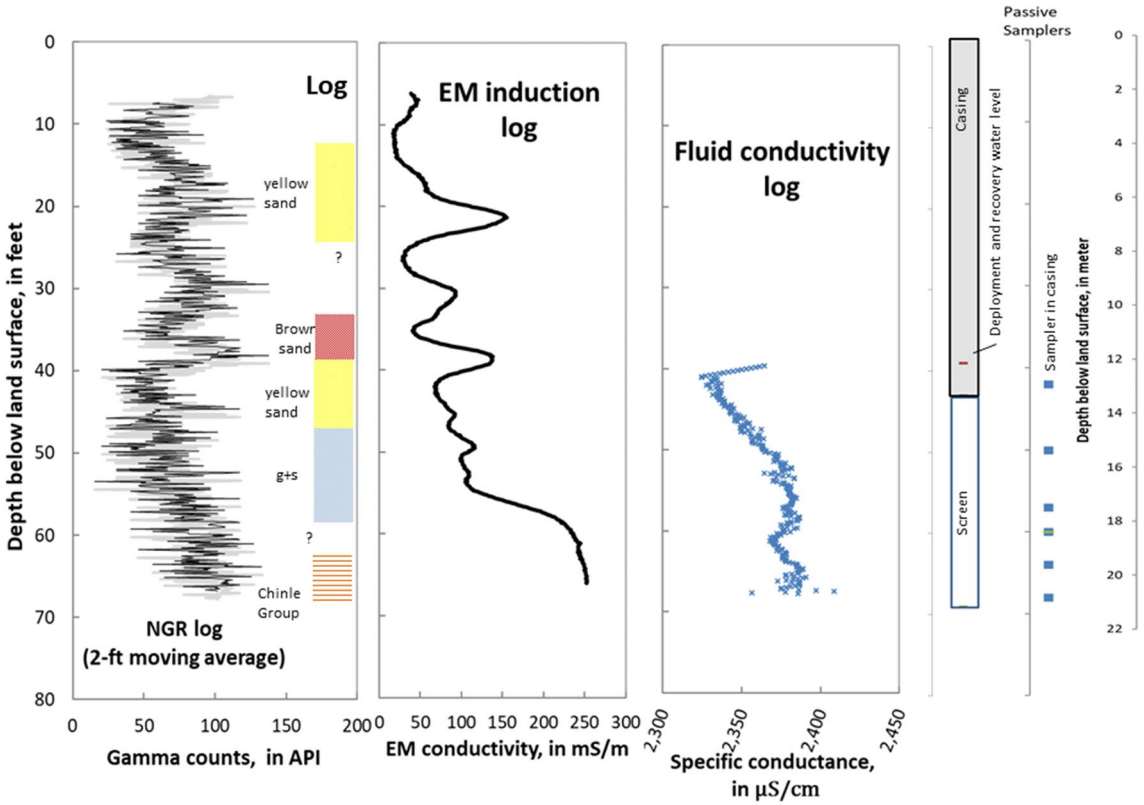

Fig. 3 Borehole geophysical logs (NGR, EM induction, and ambient fluid conductivity) and passive sampler deployment depths for well ND, Homestake Superfund site, near Milan, New Mexico [Dark line for NGR is 2-ft (0.61-m) moving average plotted with raw data (Harte et al. 2018b); *ms* medium sand, *fs* fine sand, *cg* coarse gravel, *g* gravel, *?* unknown]

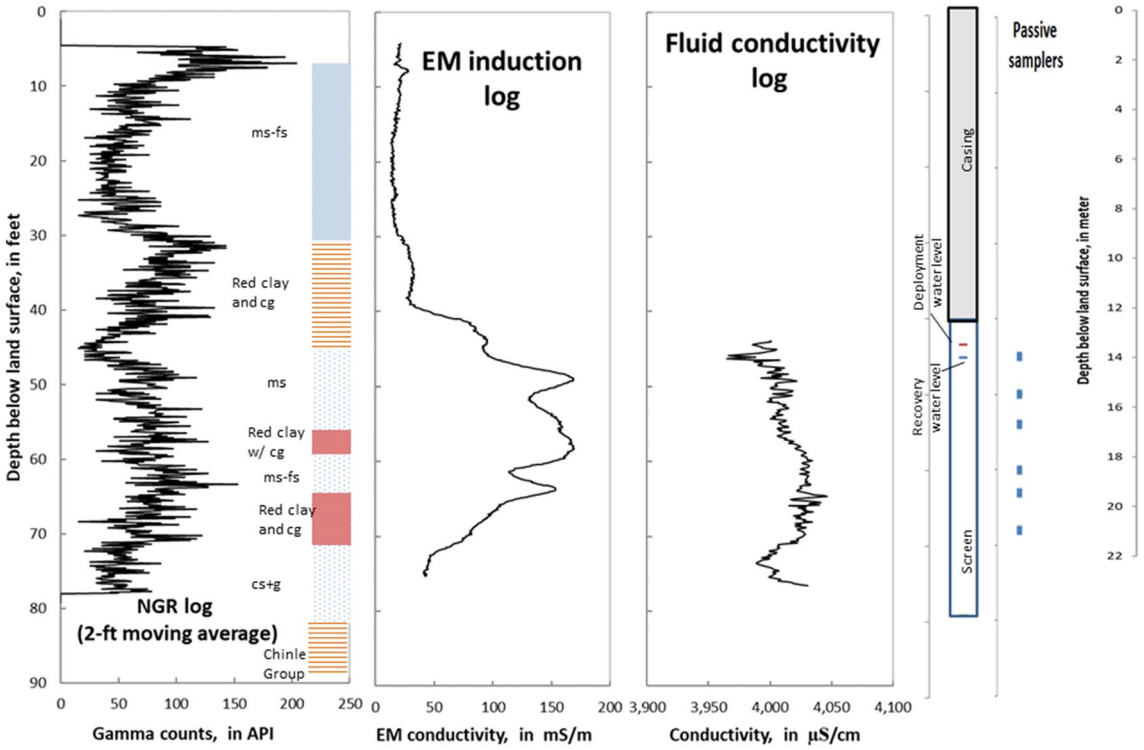

Fig. 4 Borehole geophysical logs (NGR, EM induction, and ambient fluid conductivity) and passive sampler deployment depths for well DD, Homestake Superfund site, near Milan, New Mexico. [Dark line for NGR is 2-ft (0.61-m) moving average plotted with raw data (Harte et al. 2018b); *ms* medium sand, *fs* fine sand, *cg* coarse gravel, *g* gravel]

increase in the NGR log. An increase in the NGR log also occurs at the bottom of the well in the Chinle Group. The EM induction log shows a spike in conductivity coinciding with the yellow sand (Fig. 3; depth of 42 ft or 12.8 m bls). Because that depth (42 ft or 12.8 m bls) is near the water table, trapped pore fluid likely is present near the water table. The EM induction log also shows an increase in conductivity corresponding to the Chinle Group at the bottom of the well similar to the NGR increase, indicating a formation change. The ambient fluid conductivity log, while showing generally little change in conductivity with depth in the well, shows a slight increase at the yellow sand layer (depth of 42 ft or 12.8 m bls) similar to the EM induction log, indicating a fluid change and some stratified inflow into the well.

At well DD, several of the red clay layers are associated with higher NGR counts (Fig. 4; depths of 37 ft or 11.3 m, 58 ft or 17.7 m, and 64 ft or 19.5 m bls). Parts of the medium sand (ms) (Fig. 4; ms at 50 ft or 15.2 m and 62 ft or 18.9 m bls) and the coarse sand (cs) and gravel (g) (Fig. 4; cs + g at 72 ft or 21.9 m bls) are associated with lower NGR counts. The EM induction log shows a spike near the water table in the ms layer (Fig. 4; 49 ft or 14.9 m bls) but otherwise shows relatively low EM conductivity elsewhere in the ms and cs + g layers. The fluid conductivity log shows negligible change at that same depth of 49 ft or 14.9 m bls, indicating that the EM conductivity increase is associated with a sediment change as shown by the NGR log. In contrast, both the EM induction log and fluid conductivity log show a decrease in the cs + g layer at a depth of 73 ft or 22.3 m bls, indicating fluid chemistry changes and stratified inflow, respectively (Fig. 4).

A summary of bulk geophysical characteristics per well is provided in Table 1. Well Q had the greatest difference in NGR counts (API units), whereas wells ND and DD2 the least (Table 1). In contrast, well Q had the least variability in EM conductivity whereas well T11 had the most. Wells ND and DD2 had a similar range of variability in EM conductivity. Little variation of the fluid conductivity log, like at well Q, indicates either a well-mixed aquifer or a well that is dominated by ambient flow from one layer. Larger variation in the fluid conductivity log, like at well T11, indicates chemical constituents with different electrical properties flowing into the well at different depths from a stratified inflow. Therefore, low variability in the ambient fluid conductivity log does not preclude different water chemistry external to the well with depth, as high variability often is indicative of a formation with different water chemistry with depth.

Upward ambient fluid flow was measured at well DD from the bottom of the well near the basal alluvium and

Table 1 Summary of geophysical log parameters used to assess the degree of heterogeneity of the formation and relative amount of in-well mixing, Homestake Superfund site, near Milan, New Mexico

Parameter	Units	Well name					
		Q	ND	DD	DD2	T11	MV
Difference in minimum and maximum natural gamma-ray (NGR) measurement (saturated section)	(API)	204	117	138	112	158	150
Difference in minimum and maximum electromagnetic (EM) conductivity measurement (saturated section)	(mmho/m)	4	184	129	192	219	148
Ambient fluid logs (conductivity and temperature) show variability with depth	(Y is > ±20% between minimum and maximum; otherwise N)	Y; only varied within casing but not the screen	Y	Y; only at the bottom of well	N	Y; increasing conductivity with depth	Y
Flow detected with flowmeter under ambient conditions	(Y or N)	N	N	Y; (most inflow at 73 to 64 ft bls or 22.3 to 19.5 m bls; outflow from 64 to 54 ft bls or 19.5 to 16.5 m bls)	–	–	–
Location of flow distribution measured with flowmeter under pumped conditions	Depth (ft)	Most inflow from top of screen (68 ft bls or 20.7 m bls) to 78 ft bls or 23.8 m bls	Most inflow from bottom of screen below 60 ft bls or 18.3 m bls (well screen to 64 ft bls or 19.5 m bls)	Most inflow from 62 to 72 ft bls or 18.9 to 22 m bls near the bottom of the well (well screen to 78 ft bls or 23.8 m bls)	–	–	–

– no data, *API* American Petroleum Institute units, *mmho/m* millimhos per meter, *Y* yes, *N* no, *bls* below land surface, *ft* feet, *m* meter

underlying Chinle Group by the flowmeter (Table 1). The fluid conductivity also indicates that a horizontally stratified flow takes place under ambient conditions at well DD. Flow during pumping conditions showed a preferential inflow at all three wells measured by the flowmeter (Q, ND, and DD). Well Q had an inflow near the top of the screen, whereas wells ND and DD had inflows near the bottom of the screen.

Summary statistics on the NGR log results and the SGR log results (mean K, U, and Th) are in Table 2 and provide information on gross responses per well from the radioactive signature of the lithology and mineralogy of the formation. Well MV had the lowest mean NGR counts, indicating less fine-grained sediments are present; whereas well ND had the highest mean NGR counts, indicating more fine-grained sediments are present. The standard deviation of the NGR counts was lowest in well DD2, indicating less variability, and highest in well Q. However, the lithologic logs indicate a thick clay layer and thin sand layers at wells DD and DD2 (Homestake Mining Co., written commun. 2016). Bed thickness affects the NGR response and the thin sand layers may suppress NGR responses and limit NGR variation. In well Q, the variation is due to one particular spike of NGR counts at 85 ft or 25.1 m bls [supplemental information well characteristic Table (s2)]. Well T11 had the lowest mean K of 11.6 picocuries per gram (pCi/gm) and well ND the highest mean K of 23.5 pCi/gm. The variation in U was much smaller among the wells indicating that U is ubiquitous in the alluvium and upper Chinle Group. Counts of Th were lower than counts of K and U in all wells (Table 2).

The relation between the principal radioactive elements is an indicator of the lithologic and mineralogic composition of the formation and the chemical sorption processes taking place. Individually, the NGR log and the U, K, and Th from the SGR logs are poorly correlated (Table 3) using the Pearson Product-Moment Correlation Coefficient at 95% confidence level (Helsel and Hirsch 2002). This indicates that the presence of U, K, and Th is depth specific and no bulk trend is readily observable. The exception is well T11 where NGR and U from the SGR log are well correlated, and to a lesser extent well MV; wells DD, ND, and DD2 group together. Well T11 is drilled into the LTP. K and Th from the SGR logs are generally positively correlated, and this is indicative of the presence of clay minerals such as illite (Klaja and Dudek 2016). U and Th from the SGR logs are negatively correlated as are K and U (Table 3).

In wells ND, DD, and DD2, a reddish to brown sand and clay layer was found at a depth of approximately 40 ft or 12.2 m below land surface (bls) (supplemental information s2). The water table was found immediately below this depth. The NGR and SGR logs had an increase in API and U in pCi/gm, respectively, that was associated with the layer at 40 ft or 12.2 m bls. Wells DD and DD2 had interbedded

Table 2 Summary of natural gamma-ray (NGR) and spectral gamma-ray (SGR) logging results, Homestake Superfund site, near Milan, New Mexico

Log parameter	Units	Well name					
		Q	ND	DD	DD2	T11	MV
Mean gamma (NGR)	(API)	71.4	74.7	67.3	69.6	88.1	61.3
Stdevp gamma (NGR)	(API)	34.5	25.2	24.4	20.2	32.8	33.4
Mean K-spectral (SGR)	(pCi/gm)	17.1	23.5	16.5	14.6	11.6	15
Mean U-spectral (SGR)	(pCi/gm)	3.6	3.6	3.6	3.3	3.9	2.8
Mean Th-spectral (SGR)	(pCi/gm)	2.0	2.4	1.7	1.6	1.4	1.3

API American Petroleum Institute units, *pCi/gm* picocuries per gram, *Stdevp* standard deviation of the population; data from screen opening of well

Table 3 Natural gamma-ray (NGR) and spectral gamma-ray (SGR) correlation coefficient between paired radioactive elements, Homestake Superfund site, near Milan, New Mexico

Correlation pairs	Units	Well name					
		Q	ND	DD	DD2	T11	MV
NGR to SGR-U	(API)−(pCi/gm)	0.11*	0.03*	0.00*	0.02*	0.70	0.25
NGR to SGR-K	(API)−(pCi/gm)	0.02*	0.03*	−0.27	0.10*	0.60	0.01*
NGR to SGR-Th	(API)−(pCi/gm)	0.04*	0.10*	0.14	0.02*	−0.54	0.06*
SGR-K to SGR-U	(pCi/gm)	−0.81	−0.88	−0.88	−0.79	0.68	−0.83
SGR-U to SGR-Th	(pCi/gm)	−0.86	−0.90	−0.86	−0.88	−0.77	−0.87
SGR-K to SGR-Th	(pCi/gm)	0.71	0.74	0.79	0.68	−0.43	0.78

Statistics for entire logged section of well; *U* uranium, *K* potassium, *Th* thorium, *NGR* natural gamma-ray, *SGR* spectral gamma-ray, *Correlation* Pearson Product-Moment Correlation Coefficient, *API* American Petroleum Institute units, *pCi/gm* picocuries per gram

*Not significant at the 95% confidence level

clays and sand layers along the screen interval that may promote the contact between more oxic waters from sand layers and reduced waters from clay beds, whereas wells Q and ND had less clay. It is inferred from the NGR log that well MV has a coarse-grained upper layer overlying a fine-grained lower layer. At well T11, the tailings pile is clearly identifiable by high NGR and U as identified in the SGR log along the upper part of the well above the water level depth of 100 ft or 32.8 m bls.

Sampling results

Comparison of sampling

Harte et al. (2018a) showed that the aqueous U and Se concentration results from the NS passive samplers were consistently underestimated in comparison to the purge (micropurge or volumetric) sample concentrations; however, the relation between the two methods was linear. This relation allowed for a correction to be applied to the concentration results for the passive samplers (Harte et al. 2018a). The ratio of concentrations between the passive and purge samples was 0.2811 for U and 0.2888 for Se. All passive sampler concentrations reported in this paper were adjusted by a factor of 3.55 (1/0.2811) for U and a factor of 3.46 (1/0.2888) for Se to adjust results to an equivalent micropurge concentration, according to the methods described by Harte et al. (2018a). These adjustment factors are consistent with the diffusion rates of U and Se, deployment times, and dimensions of the samplers as identified in supplemental information presented with this paper (s3, s4).

U concentration results from the three different sampling methods at the six monitoring wells are summarized in Table 4. The U concentrations from the volumetric and micropurge samples are in close agreement. The 6 volumetric samples from the 6 wells and the 7 micropurge samples (2 micropurge samples were collected at well DD2) from the 6 wells yielded similar concentrations indicating that well water within the screen under ambient conditions is representative of the formation. The micropurge samples are instantaneous samples collected without inducing well inflow from pumping and therefore represent the in-situ water in the screen at that interval. Volumetric sampling, which requires large amounts of purging, is, therefore, not needed to collect a representative sample. The largest difference (56 µg/L) between the volumetric (297 µg/L) and micropurge (353 µg/L) samples is from well MV. The volumetric sample at well MV was collected at 71 ft or 21.6 m bls (near bottom of casing and top of well screen) and the micropurge sample was collected at 82 ft or 25 m bls, within the screen interval. The vertical profile of U from well MV shows a net increase of 60 µg/L with depth from 67 to 82 ft or 20.4 to 25 m bls (Harte et al. 2018a). We conclude that the volumetric sample for well MV captures some water from the well casing based on relative concentration differences from the vertical profile of U.

The variability in concentrations from the passive sampling profile can be identified by the relative magnitude of the standard deviation of U concentrations from the passive samplers (Table 4). The concentration of U for passive sampling shows small variation at 2 of the wells profiled (wells ND and Q; Table 4) and larger variations at 4 of the wells (wells MV, DD, DD2, T11; Table 4). Well T11 had the highest mean U concentration and largest standard deviation from the profile of passive samplers and is located at the LTP (Fig. 1b). Based on the trend of the profile (Fig. 7), we attribute the variability to differences in lateral transport of U from different parts of the LTP. Well ND had the lowest mean U concentration but not the lowest standard deviation from the profile of passive samplers and is located northeast of the LTP (Fig. 1b). Well Q had the smallest standard deviation that indicates that the well and potentially the formation is well mixed with little vertical variation in U concentrations in groundwater. Wells DD, DD2, and MV are located proximal to the LTP (Fig. 1b). Despite the proximity to well DD, well DD2 water had a larger variation in U concentrations than well DD water. Wells ND and Q are screened in predominantly silt and sands, whereas wells DD and DD2 are screened in interbedded clays and silts and sands. Well MV is screened in sands and is located downgradient from the LTP and likely receives U groundwater transport from the LTP.

Physical heterogeneity of the alluvium likely affects the U concentration variability. The interbedded clays at wells DD and DD2 may contain reduced waters where U in the form of U(IV) may be sorbed onto sediments and in proximity to oxic waters that induce mobilization of U by converting U(IV) to mobile U(VI). Where there are primarily sands and silts (wells ND and Q), the aquifer is well mixed and has less U variability.

Concentrations of U in groundwater, excluding that in well T11, varied by one order of magnitude, ranging from 25 (well ND) to 297 µg/L (well MV) in volumetric samples, 31 (well ND) to 353 µg/L (well MV) in micropurge samples, and the mean passive sample from the chemical profiles varied from 24 (well ND) to 313 µg/L (well MV) (Table 4). Individual passive sampler concentrations ranged from 12 (well ND) to 351 µg/L (well MV) (Harte et al. 2018a). In wells where casing water was present and passive samplers were set in the casing water (wells MV, Q, and DD2), the U concentrations were lower than the concentration of the passive samplers set in the screens (Table 4).

Table 4 Summary of aqueous uranium (U) concentrations [micrograms per liter (µg/L)] from multiple types of sampling methods including passive sampling, Homestake Superfund site, near Milan, New Mexico

Type of sample	Parameter	Sample description	Units	Well name						
				ND	MV	Q	DD	DD2	DD2	T11
Volumetric	Total uranium	Sample collected after evacuation of three well volumes	(µg/L)	25	297	**66**	**103**	250	–	10,677
	Sample depth below LSD		(ft)/(m)	49/14.9	71/21.6	68/20.7	54/16.5	50/15.2	–	140/42.7
Micropurge	Total uranium	Sample collected after evacuation of pump and hose volume	(µg/L)	**31**	**353**	61	90	**263**	**257**	10,353
	Sample depth below LSD		(ft)/(m)	64/19.5	82/25	88/26.8	54/16.5	72/22	60/18.3	140/42.7
[a]Passive	Number of samples			7	9	9	7	12	–	11
	Mean total uranium	Mean concentration from profile of passive samples including casing sample	(µg/L)	24	313	53	[b]65	167	–	16,508
	Total uranium	Passive sample located within casing (casing sample)	(µg/L)	None	238	46	None	44	–	None
	Mean total uranium	Mean concentration from profile of passive samples excluding sample from casing zone	(µg/L)	24	322	54	[b]65	180	–	16,508
	Standard deviation of total uranium	Excludes passive sample from casing zone	(µg/L)	6.4	23.4	3.7	[b]23.8	50.5	–	7502

Bold highest value between volumetric and micropurge sample, *none* no sample, – use previous value from same well, *LSD* land surface datum, *ft* feet, *m* meter, Uranium concentrations from Harte et all. (2018a)

[a]Passive sampler concentrations were adjusted by a factor 3.55 (1/0.2811) for U according to Harte et al. (2018a)

[b]Uppermost sampler possibly exposed due to shallow water levels

Table 5 Summary of aqueous Se concentrations [micrograms per liter (µg/L)] from multiple types of sample methods including passive sampling, Homestake Superfund site, near Milan, New Mexico

Type of sample	Parameter	Sample description	Units	Well name						
				ND	MV	Q	DD	DD2	DD2	T11
Volumetric	Total selenium	Sample collected after evacuation of three-well volumes	(µg/L)	**150**	**35**	**460**	130	**13**	–	180
	Depth of sample below LSD		(ft)/(m)	49/14.9	71/21.6	68/20.7	54/16.5	50/15.2	–	140/42.7
Micropurge	Total selenium	Sample collected after evacuation of pump and hose volume	(µg/L)	51	29	380	**170**	2	**8**	**350**
	Depth of sample below LSD		(ft)/(m)	64/19.5	82/25	88/26.8	54/16.5	72/22	60/18.3	140/42.7
[a]Passive	Number of samples			7	9	9	7	11	11	12
	Mean total selenium	Mean concentration from profile of passive samples including casing sample	(µg/L)	65	26	408	[b]152	6	–	121
	Total selenium	Passive sample located within casing (casing sample)	(µg/L)	None	15	381	None	< 1.5	–	None
	Mean total selenium	Mean concentration from profile of passive samples excluding casing sample	(µg/L)	65	28	411	[b]152	13	–	121
	Standard deviation of selenium	Exclude sample from casing	(µg/L)	23.7	8.2	20.8	[b]23.7	3.3	–	75.1

Bold highest value between volumetric and micropurge sample, *none* no sample, – use previous value from same well; LSD means land surface datum, *ft* feet, *m* meter

[a]Passive sampler concentrations were adjusted by a factor of 3.46 (1/0.2888) for Se according to Harte et al. (2018a)

[b]Uppermost sampler possibly exposed due to shallow water levels

Aqueous Se concentration results from the three different sampling methods in the six monitoring wells are summarized in Table 5. The 6 volumetric samples from the 6 wells and the 7 micropurge samples from the 6 wells yielded similar concentrations in 4 of the 6 wells.

The relatively variability of Se, like the relative variability of U, is high at wells T11 and MV; these wells are likely influenced by local anthropogenic sources of contamination. In two wells (ND and Q) that show little variation in U concentration (Table 4), the Se concentration shows a greater variability (Table 5). Well DD2 has some variability in U concentrations but little variability in Se concentrations (Table 5). Se like U is affected by redox conditions and Se (and U) is less mobile under reducing conditions. Well DD2 had low dissolved oxygen (D.O.) concentrations [< 1 milligram per liter (mg/L)] and low Se concentrations (Harte et al. 2018b). In contrast, well DD located near well DD2 had higher D.O. concentration (3.9 mg/L), and Se concentrations were higher at well DD than well DD2 (Table 5). Well Q, despite showing little variability in U concentrations, had a greater variability in Se concentrations. In wells where casing water was present and passive samplers were set in the casing water (wells MV, Q, and DD2), the concentrations were typically lower than the concentration of the passive samplers set in the screens (Table 5). The exception was in well MV where the Se concentration (6 µg/L) was lowest at the lowermost sampler (102 ft or 31.1 m bls; Harte et al. 2018a) and may represent concentrations more indicative of groundwater from the Chinle Group than the other samplers in that well.

U and Se from passive samplers

The co-occurrence of aqueous U and Se concentrations is used here as a marker of anthropogenic sources of contamination. We used the co-occurrence of aqueous U and

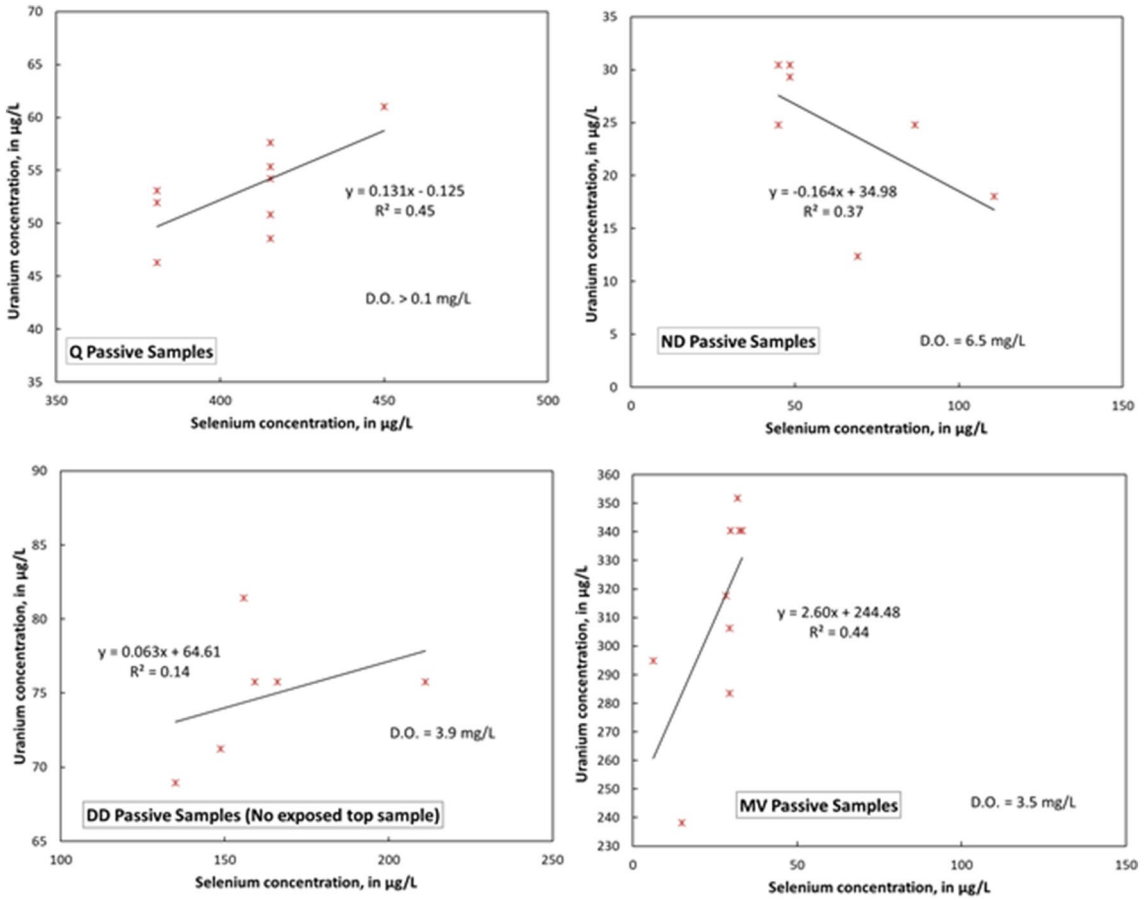

Fig. 5 Cross plots of aqueous U and Se concentrations in micrograms per liter (µg/L) from passive samplers, Homestake Superfund site, near Milan, New Mexico [U and Se concentrations were adjusted according to Harte et al. (2018a); dissolved oxygen (D.O.) concentration given in milligrams per liter (mg/L)]

Se concentrations from the passive samplers to provide a larger population to evaluate well specific trends. Results are shown for wells DD, ND, Q, and MV to highlight contrasting results (Fig. 5). A particularly poor regression of co-occurrence concentrations provides insight into whether the anthropogenic signal is weak. Linear regression of U and Se concentrations for wells DD [coefficient of determination (R^2) = 0.14; probability value (p) = 0.46; Fig. 5] and DD2 (R^2 = 0.28; p = 0.09; not shown) shows weak relations that are not statistically significant at the 95% confidence interval. Well T11 (not shown) also had a poor R^2 (0.06) due to the large range of U concentrations at the LTP. In contrast, linear regression of U and Se concentrations had the highest R^2 for well Q (R^2 = 0.45; p = 0.05) and well MV (R^2 = 0.44; p = 0.05). These wells are interpreted as being affected by regional milling operations for well Q and local operations (Site) for well MV given their locations. Therefore, both sources of U contamination have signatures of Se contamination. Well ND shows an inverse relation with an R^2 of 0.37 (p = 0.14). We interpret this as the effect of upwelling of Chinle Group waters that have relatively higher U and lower Se concentrations than the alluvial aquifer at this location.

One-half of the six wells have a discernible trend in Se and U vertical concentration profiles as measured by the passive samplers (Figs. 6, 7). The trend is most discernible in well T11 and, although drilled through the LTP, the increasing trend in depth with Se and U indicates that lateral transport of these contaminants is affecting concentrations in this well rather than vertical transport alone. The borehole geophysical logs for T11 indicate a permeable layer in the Chinle Group at an approximate depth of 180 ft or 54.9 m bls that appears to be transporting contaminants (Harte et al. 2018a).

Comparison of passive sampling and borehole geophysical logs

The bulk gamma response from the NGR log compares poorly to U and Se concentrations (Table 6). This may in part be related to anthropogenic sources and transport of

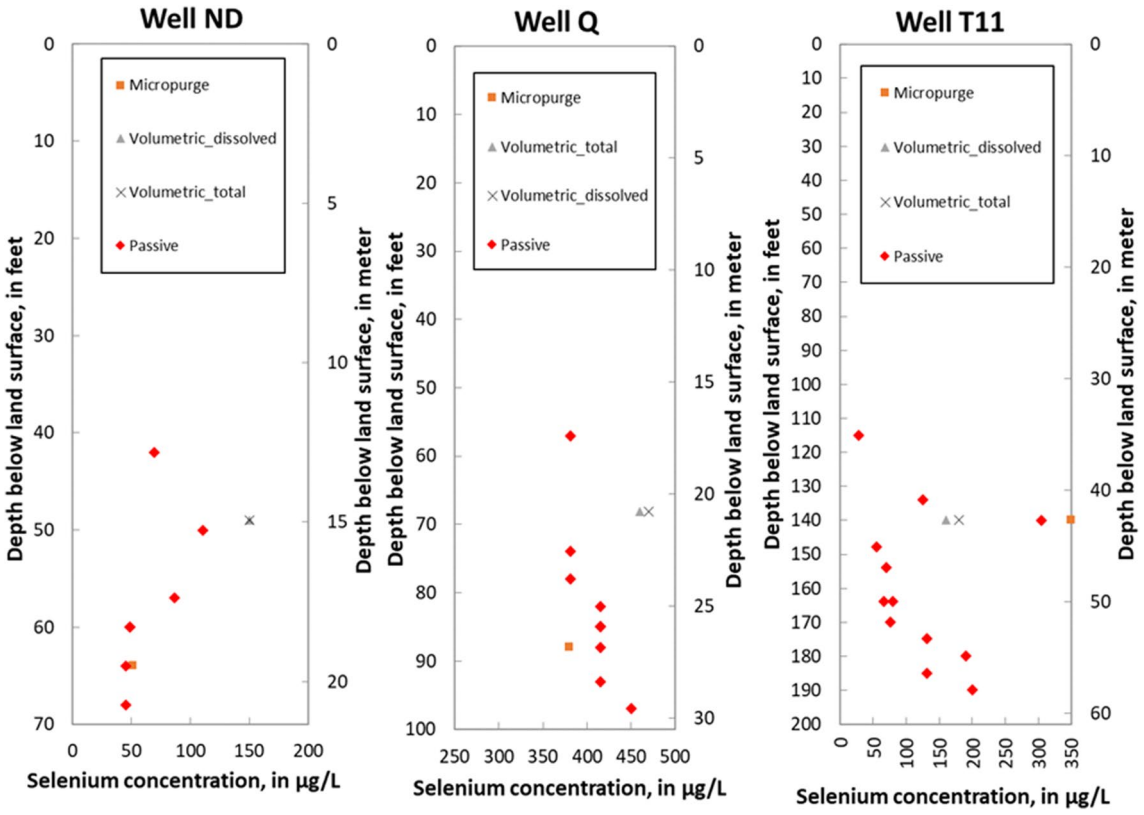

Fig. 6 Vertical profiles of aqueous Se concentrations from passive samplers and concentrations from purge (micropurge and volumetric) samples, Homestake Superfund site, near Milan, New Mexico [Aqueous U and Se concentrations were adjusted according to Harte et al. (2018a)]

U affecting well water concentrations, such as in wells Q (regional mills/mining), MV (local Homestake milling operation), and T11 (local Homestake milling operation). Further, mixing of Chinle Group waters may affect U and Se concentrations in water from several wells (ND, DD, DD2, and T11). The two wells that sample primarily alluvial aquifer waters, wells Q and MV, are affected by anthropogenic sources and transport of U. Therefore, there are no wells from our sample group that can be used to help identify natural sources of U in the alluvial aquifer waters alone because most are affected by mixing of some Chinle Group waters.

K and Th appear to be a better predictor of aqueous U concentrations than NGR or U from the SGR log (trolling measurements) based on regression. The mean aqueous U concentration from the passive samplers per well was plotted against the mean K, Th, and U from the SGR log per well (Fig. 8). An inverse relation is apparent between increasing K and Th from the SGR logs and the decreasing mean aqueous U concentration. We attribute the inverse relation to the presence of clays and its effect on the sorption of aqueous U and redox (tendency for more reduced conditions). The stacked measurements for Th also show an inverse trend (not shown; Harte et al. 2018b).

Discussion

The screen lengths of the 6 monitoring wells tested for this study are relatively long (> 20 ft or > 6.1 m) and intersect a heterogeneous aquifer of interbedded sands, silts, and clays (in some wells). The heterogeneity of the alluvium is identifiable by the variability in results of borehole geophysics measurements of NGR, SGR, and EM induction logs. The degree of mixing of groundwater is identifiable with the EM induction and fluid (conductivity and temperature) logs. The EM induction log was used to assess the degree of mixing in the formation, whereas the fluid logs were used to assess the degree of mixing in the well.

If the fluid log (either conductivity or temperature) showed a variation with depth so too did the vertical profile for chemistry for either U or Se concentrations from passive samplers; the exception was well DD2 that showed little fluid log variability but some variability in the vertical profile of U concentrations. We attribute the variability in aqueous U concentrations to depth-dependent redox processes. Iron-staining on the NS passive samplers from the exposure of oxygenated water in passive samplers to reduced waters in the well occurred in more than one-half of the samplers; this indicates

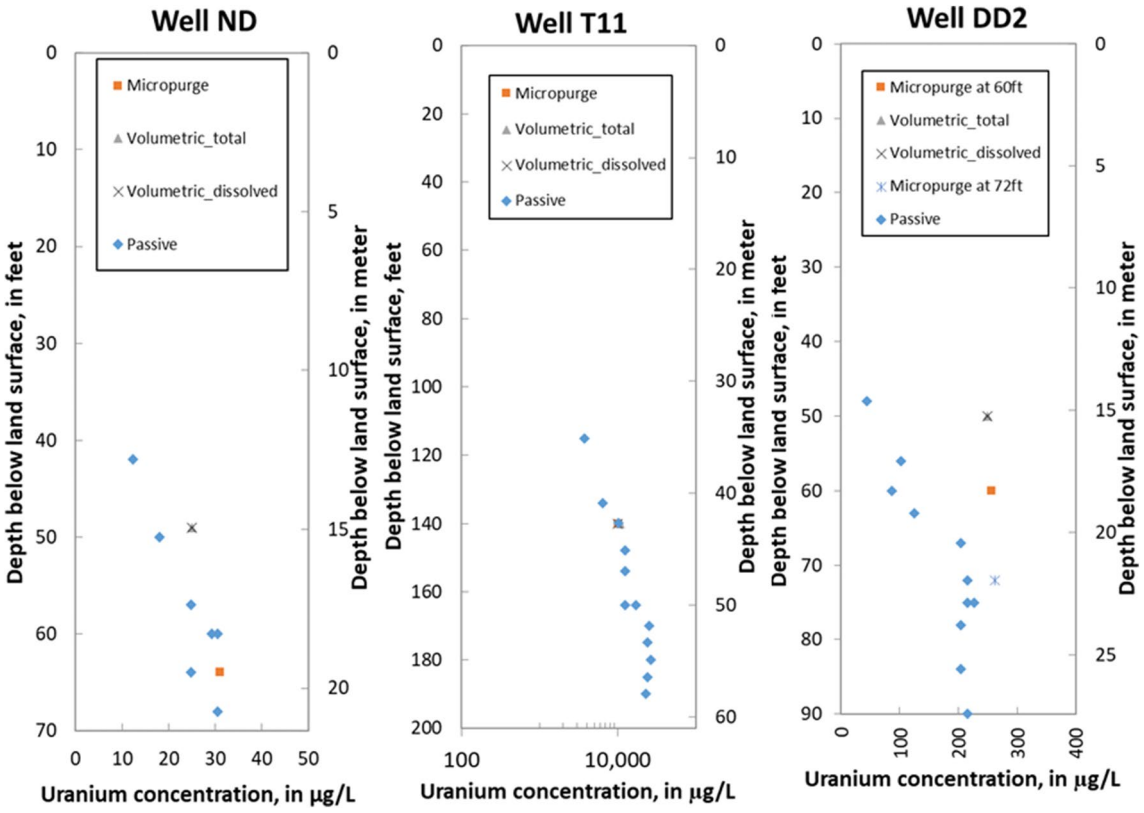

Fig. 7 Vertical profiles of aqueous U concentrations from passive samplers and concentrations from purge (micropurge and volumetric) samples, Homestake Superfund site, near Milan, New Mexico [Aqueous U and Se concentrations were adjusted according to Harte et al. (2018a)]

Table 6 Variation of natural gamma-ray (NGR) and spectral gamma-ray (SGR) to variation of aqueous U concentration from passive samplers, Homestake Superfund site, near Milan, New Mexico

Log	Units	Well name					
		Q	ND	DD	DD2	T11	MV
Mean gamma (NGR)	(API)	71.4	74.7	67.3	69.6	88.1	61.3
Stdevp gamma (NGR)	(API)	34.5	25.2	24.4	20.2	32.8	33.4
Mean K-spectral (SGR)	(pCi/gm)	17.1	23.5	16.5	14.6	11.6	15
Mean U-spectral (SGR)	(pCi/gm)	3.6	3.6	3.6	3.3	3.9	2.8
Mean Th-spectral (SGR)	(pCi/gm)	2.0	2.4	1.7	1.6	1.4	1.3
Mean concentration of U from the profile of passive samples excluding casing sample	(µg/L)	54.0	24	65	180	16,508	322
Standard deviation of U concentration from the profile of passive samplers excluding casing sample	(µg/L)	3.7	6.4	23.8	50.5	7,502.0	23.4
Mean concentration of Se from the profile of passive samples excluding casing sample	(µg/L)	411	65	163	13	121	28
Standard deviation of Se concentration from the profile of passive samplers excluding casing sample	(µg/L)	20.8	23.7	23.7	3.3	75.1	8.2

API American Petroleum Institute units, *pCi/gm* picocuries per gram, *µg/L* micrograms per liter, U and Se concentrations adjusted by Harte et al. (2018a)

that stratified inflow occurs. The most reduced waters would have the largest amount of ferrous iron precipitate onto the NS mesh of the sampler given that oxic water was used within the samplers promoting iron staining on the mesh.

Most of the wells capture mixed water from the alluvial aquifer and underlying Chinle Group; results show that only wells Q and MV primarily capture water from the alluvial aquifer. All the wells except for well Q are screened within

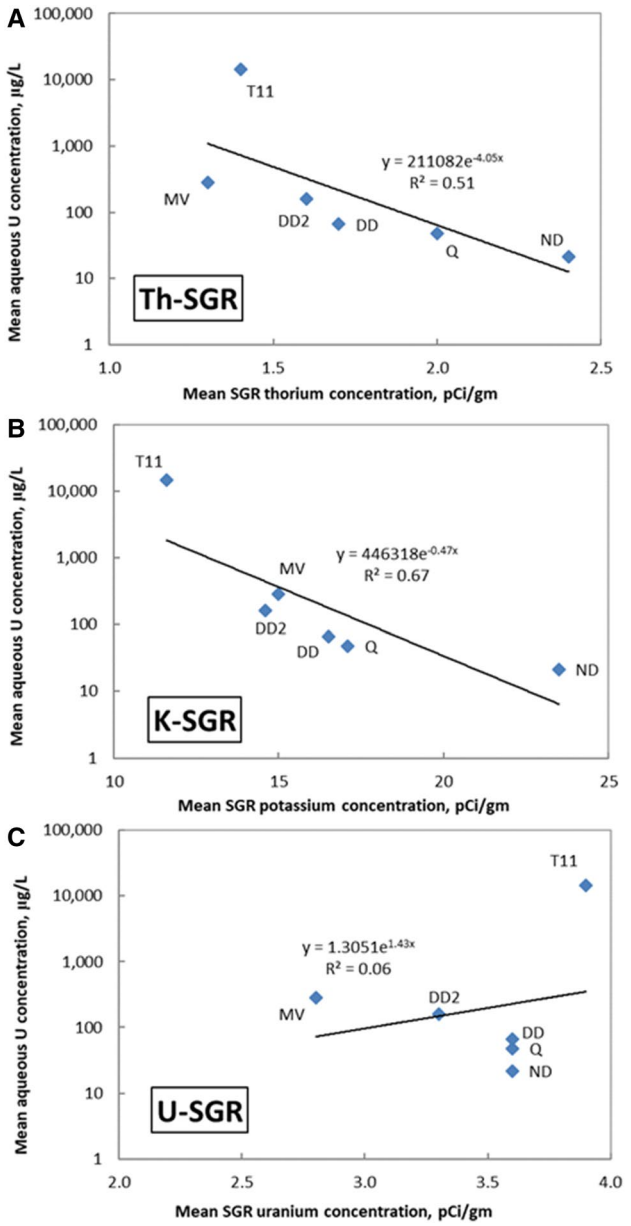

Fig. 8 Comparison of mean aqueous uranium (U) concentrations in micrograms per liter (µg/L) from passive samplers and mean spectral gamma-ray (SGR) measurements for thorium, potassium, and uranium in picocuries per gram (pCi/gm) for the screen opening of well, Homestake Superfund site, near Milan, New Mexico (Aqueous U and Se concentrations were adjusted according to Harte et al. 2018a)

or immediately overly the underlying Chinle Group. The lithologic log for well MV is not available from the drilling record but based on the response of the NGR log, it is likely that this well is also drilled into the Chinle Group. Wells ND, DD, DD2, and T11 capture Chinle Group waters in addition to alluvial aquifer waters. Therefore, water samples reflect a mixture of alluvial aquifer and underlying Chinle Group waters. In some cases, the amount of water being derived from the Chinle Group may be small relative to the alluvial aquifer water (e.g. well MV) yet contact with the Chinle Group may affect the geochemistry of the well water.

For aqueous U concentrations, the effect of capturing groundwater from the Chinle Group is dependent on the location of the well and whether the alluvial aquifer water U concentrations are relatively low (< 100 µg/L) or high (> 300 µg/L) at that location. Wells in the Chinle Group had concentrations of approximately 100–300 µg/L (Harte et al. 2018b). For aqueous Se concentrations, the addition of groundwater from the Chinle Group would tend to decrease concentrations. The influence of mixing of waters in the alluvium with upwelling of Chinle Group waters is visible at well ND. This well had an inverse profile trend in aqueous U concentration (increasing with depth) and aqueous Se concentration (decreasing with depth), which is indicative of an up flow of Chinle Group waters at this location. Analysis of time-varying capture during volumetric sampling (supplemental information s5) also supports this interpretation. In well DD2, aqueous Se concentrations are very low and can be attributed to upflow of Chinle Group waters or fault waters given its proximity to a fault (Fig. 1b). Alternatively, the low aqueous Se concentrations could also be attributed to early precipitation or sorption of Se on U roll-front type deposits (Brookins 1977). Selenium adsorption can be associated with iron hydroxides, which were visually observed on the NS mesh of the passive samplers.

A high U (pCi/gm) from the SGR logging was sometimes associated with high NGR (API). A high U (> 5 pCi/gm) was found in red clays, other clay layers, brown sand, and in the basal alluvium and the underlying Chinle Group (Harte et al. 2018b). The mean U varied per well from a low of 2.8 pCi/gm in well MV to a high of 3.6 pCi/gm at wells Q, ND, and DD (Table 6). The narrow range of mean U concentration per well from the SGR indicates that U is ubiquitous in the alluvium and Chinle Group. However, K was the dominant radioactive element present. K varied from a low of 11.6 pCi/gm in well T11 to a high of 23.5 pCi/gm in well ND. Thorium and its relation to K is an indicator of clay mineralogy (Klaja and Dudek 2016). Thorium varied from a low of 1.3 pCi/gm (mean) in well MV to a high of 2.4 pCi/gm (mean) in well ND.

The mean Th as measured by the SGR logs was found to generally inversely relate to the mean aqueous U concentrations from the vertical profile of the passive samplers. This is an indicator of the presence of clays, reduced conditions, and U sorption. The higher the Th, the more likely that clays are present, and the greater the tendency for reduced conditions to be present.

Almost all the wells were found to contain some proximal source of U based on the SGR logs. The proximal source of U can be from the natural U occurrence or enrichment of U that was likely transported in groundwater from an

anthropogenic source and later sorbed. Wells likely affected by anthropogenic transport source of U from a distal location include wells Q and MV; well T11 is affected by a local anthropogenic source (LTP) of U.

Uranium isotope ratios of $^{234}U/^{238}U$ were low, suggesting a higher anthropogenic signature, at wells T11 (1.01), MV (1.07), and Q (1.18) as found by Harte et al. (2018b). Wells MV and Q had a relatively high relation of co-occurrence of aqueous U and Se concentrations from passive samplers indicating an anthropogenic signature. Uranium isotope ratios were higher, indicating a lower anthropogenic signature, in wells DD (1.53), DD2 (1.48), and ND (1.43). Wells with a ratio greater than 1.3 may be potentially unaffected by an anthropogenic U source or conversely subjected to upwelling and mixing of Chinle Group waters. Mixing of Chinle waters is likely based on this work at alluvial aquifer wells (DD, DD2, and ND). Therefore, relatively high $^{234}U/^{238}U$ ratios can be produced from the mixing of relatively low $^{234}U/^{238}U$ ratio alluvial waters and the mixing and the upwelling of Chinle Group waters with relatively high ratios. Waters from the Chinle Group had ratios > 2 in samples from several wells at the Site (Harte et al. 2018b). Therefore, a well that intersects a formation affected by milling could have a U isotope ratio indicative of U milling, which is typically a $^{234}U/^{238}U$ ratio near 1 but also intersect another formation unaffected by milling with a ratio of 2, which is indicative of unaltered U (Zielinski et al. 1997). If evenly mixed the resultant well water would have a ratio of 1.5.

Conclusion

Uranium (u) is fairly ubiquitous in the alluvial aquifer and underlying Chinle Group in the lower San Mateo Creek Basin near the Homestake Mining Co. Superfund site (Site). Uranium, as measured by SGR logging had similar values of pCi/gm in all 6 monitoring wells set in the alluvial aquifer and the Chinle Group. The exception was well T11 drilled through the LTP. The highest U concentrations (> 100 pCi/gm) from the SGR log were observed above the groundwater table in the tailings as detected in well T11. In two other monitoring wells, relatively high U (> 5 pCi/gm) were also found above the water table (wells DD and DD2).

Aqueous U concentrations appear to be inversely related to Th as measured by the SGR log. This indicates the possibility that U is bound in the clays, likely through sorptive processes. This may be partly redox related given the presence of clays and less oxic conditions, while unconfirmed, likely coexist. The reduced state of U, U(IV) is less mobile in groundwater than U(VI).

In wells DD and DD2, interbedded sands and clays may provide a role in exposing oxic waters to reduced waters from the clay beds where U is likely immobile. The result would be the mobilization of U from the reduced form of U(IV) to U(VI). Core samples of formation would provide additional insight into this hypothesis.

Co-occurrence of U and Se aqueous concentrations provided insight into anthropogenic sources of U from mine and milling waste. Two of the wells, Q from regional mine/milling waters and MV likely from local milling waters, had the strongest relation between U and Se co-occurrence. One well, ND, showed an inverse relation indicating Chinle Group waters with relatively high U and low Se concentrations are upwelling into the well. Wells DD and DD2 showed a poor relation between U and Se and therefore show a relatively poor fingerprint of an anthropogenic source of U. However, in well DD2, the low Se concentrations could also be indicative of preferential Se sorption with iron-hydroxides as part of a roll-front type depositional process, which would obscure the relation with U. The interbedded sequence of clays and sand at that location could promote such a process.

More accurate determination of ambient U concentrations in the alluvial aquifer would benefit from monitoring wells with (1) shorter screens and less mixing of groundwater, and (2) targeted sampling of discrete units in the alluvial aquifer. For example, wells specifically screened in clay or sand layers, removed from direct contact with Chinle Group waters would allow for an improved determination of U concentrations for the alluvial aquifer from natural U sources. From the existing wells in this study, it was demonstrated that volumetric sampling methods were not needed to collect a representative sample from the formation and that volume-limited sampling methods, such as micropurge, is sufficient. Further, volume-limited sampling methods (conjunctive use of micropurge and passive sampling) can provide additional insight into the variability of U concentrations at the well scale.

Acknowledgements The authors would like to thank Sai Appaji, former Remedial Project Manager, U.S. Environmental Protection Agency, Region 6, for his assistance as he oversaw project management of the Homestake Superfund site. Mr. Appaji facilitated site access to wells and helped coordinate our field activities. Mark Purcell, current Remedial Project Manager, U.S. Environmental Protection Agency, Region 6, provided information on site conditions that helped our work. Pat Longmire of the New Mexico Environment Department provided input on several aspects of the study design with the help of Kurt Vollbrecht, Program Manager for the New Mexico Environment Department. Site employees for the Homestake Mining Company also were very helpful in providing access to wells on company land. Landowners adjacent to the site supported our work before and during the data collection process. Any use of trade, firm, or product names is for descriptive purposes only and does not imply endorsement by the U.S. Government.

References

Alam MS, Cheng T (2014) Uranium release from sediment to groundwater: influence of water chemistry and insights into release mechanisms. J Contam Hydrol 164:72–87. https://doi.org/10.1016/j.jconhyd.2014.06.001

American Society of Testing and Materials (ASTM) (2004) Standard guide for conducting borehole logging—mechanical caliper. American Society of Testing and Materials (ASTM) D 6767–97, p 6

American Society of Testing and Materials (ASTM) (2007) Standard guide for planning and conducting geotechnical borehole geophysical logging. (ASTM) D5753

American Society of Testing and Materials (ASTM) (2010) Standard guide for conducting borehole geophysical logging – Gamma. (ASTM) D6274–10

Bailey RT, Hunter WJ, Gates TK (2012) The influence of nitrate on selenium in irrigated agricultural groundwater systems. J Environ Qual 41(3):783–792

Balistrieri LS, Chao TT (1990) Absorption of selenium by amorphous iron oxyhydroxide and manganese dioxide. Geochim Cosmochim Acta 54:739–751

Basu A, Brown S, Christensen JN, DePaolo DJ, Reimus PW, Heikoop JM, Woldegabriel G, Simmons AM, House BM, Hartmann M, Maher K (2015) Isotopic and geochemical tracers for U(VI) reduction and U mobility at an in situ recovery U mine. Environ Sci Techn 49(10):5939–5947. https://doi.org/10.1021/acs.est.5b00701

Boult KA, Cowper MM, Heath TG, Sato H, Shibutani T, Yui M (1998) Towards and understanding of sorption of U(VI) and Se(IV) on sodium bentonite. J Contam Hydrol 35:141–150

Brookins DG (1977) Uranium deposits of the Grants Mineral Belt: geochemical constraints on origin. Exploration Frontiers of the Central and Southern Rockies. Mineral Deposita 17:337–352

Canadian Well Logging Society (2013) LAS information–Log ASCII Standard (LAS) software. http://www.cwls.org/las_info.php. Accessed 13 May 2013

Century Geophysical LLC (2017) http://www.century-geo.com/. Accessed 22 Feb 2018

Dong W, Brooks SC (2006) Determination of the formation constants of ternary complexes of uranyl and carbonate with alkaline earth metals (Mg^{2+}, Ca^{2+}, Sr^{2+}, and Ba^{2+}) using anion exchange method. Environ Sci Techn 40(15):4689–4695. https://doi.org/10.1021/es0606327

Dubrosvky NM, Neil JM, Fugii R, Oremland RS, Hollibaugh JT (1990) Influence of redox potential on selenium distribution in ground water, Medota Western San Joaquin Valley, California. US Geol Sur Open-File Report 90–38:24

Ehrenberg SN, Svånå TA (2001) Use of spectral gamma-ray signature to interpret stratigraphic surfaces in carbonate strata: an example from the Finnmark carbonate platform (Carboniferous-Permian), Barents Sea. Am Assoc Pet Geol Bull 85(2):295–308. https://doi.org/10.1306/8626C7C1-173B-11D7-8645000102C1865D

Fabricius ID, Fazladic LD, Steinholm A, Korsbech U (2003) The use of spectral natural gamma-ray analysis in reservoir evaluation of siliciclastic sediments: a case study from the Middle Jurassic of the Haral Field, Danish Central Graben. Geol Soc Denmark Greenl Bull 1:349–366

Gallaher BM, Cary SJ (1986) Impacts of uranium mining on surface and shallow ground waters, Grants Mineral Belt, New Mexico. New Mexico Environmental Improvement Division, EID/GWH-86/2, p 152

Gallaher BM, Goad MS (1981) Water-quality aspects of uranium mining and milling in New Mexico. In: Wells SG, Lambert W, Callender JF (eds) Environmental geology and hydrology in New Mexico, vol 10. Geological Society Special Publication, Socorro, pp 85–91. http://geoinfo.nmt.edu/publications/nmgs/special/10/. Accessed 1 May 2017

Gates TK, Cody BM, Donnelly JP, Herting AW, Bailey RT, Price JM (2009) Assessing selenium contamination in the irrigated stream-aquifer system of the Arkansas River, Colorado. J Environ Qual 28:2344–2356

Hall SM, Mihalasky MJ, Tureck KR, Hammarstrom JM, Hannon MT (2017) Genetic and grade and tonnage models for sandstone-hosted roll-type uranium deposits, Texas Coastal Plain, USA. Or Geol Rev 80:716–753. https://doi.org/10.1016/j.oregeorev.2016.06.013

Harte PT, Blake JMT, Becher KD (2018a) Determination of representative uranium and selenium concentrations from groundwater, 2016, Homestake Mining Company Superfund Site, Milan, New Mexico. US Geol Survey Open-File Report 2018–1055:39. https://doi.org/10.3133/ofr20181055

Harte PT, Blake JMT, Becher KD, Thomas JV, Stengel VG (2018b) Data associated with uranium background concentrations at Homestake Mining Company Superfund site, near Milan, New Mexico, July 2016 through October 2016 (ver. 1.2, September 2018). US Geol Sur data release. https://doi.org/10.5066/F7CR5RJS. Accessed 9 Oct 2018

Helsel DR, Hirsch RM (2002) Statistical methods in water resources. US Geol Sur techniques of water-resources investigations of the United States Geological Survey, Book 4, hydrologic analysis and interpretation, p 524

Homestake Mining Co (2015) Summary and discussion of groundwater background concentrations and groundwater flow for aquifers at Homestake Mining Company's Grants Reclamation Project, Grants New Mexico, July 2015. Homestake Mining Co. of California, p 110

Hydro-Engineering LLC (2001) Ground-water hydrology for support of background concentration at the Grants Reclamation Site for Homestake Mining Company of California

Kaufman RF, Eadie GG, Russell CR (1976) Effects of uranium mining and milling on ground water in the Grants Mineral Belt, New Mexico. Ground Water J 14(5):296–308

Keys WS (1990) Borehole geophysics applied to ground-water investigations: U.S. Geological Survey Techniques of Water-Resources Investigations book 2, chap. E2, p 150

Klaja J, Dudek L (2016) Geological interpretation of spectral gamma ray (SGR) logging in selected boreholes. Nafta-GAZ, ROK LXXII 1:3–14. https://doi.org/10.18668/NG2016.01.01

Kulp T, Pratt LM (2004) Speciation and weathering of selenium in Upper Cretaceous chalk and shale from South Dakota and Wyoming, USA. Geochim Cosmochim Acta 68(18):3687–3701. https://doi.org/10.1016/j.gca.2004.03.008

Langman JB, Sprague JE, Durall RA (2012) Geologic framework, regional aquifer properties (1940s–2009), and spring, creek, and seep properties (2009–10) of the upper San Mateo Creek Basin near Mount Taylor, New Mexico. US Geol Sur Sci Inv Rep 2012–5019:96

Langmuir D (1978) Uranium solution-mineral equilibria at the temperatures with application to sedimentary ore deposits. Geochem Cosmochim Acta 42:547–569

Martin TD (2003) Determination of trace elements in drinking water by axially viewed inductively coupled plasma-atomic emission spectrometry: U.S. Environmental Protection Agency Report EPA. EPA/600/R-06/115, Revision 4.2, p 36

Masscheleyn PH, Dealune RD, Patrick WH Jr (1990) Transformations of selenium as affected by sediment oxidation-reduction potential and Ph. Environ Sci Techn 24:91–96

Mast MA, Mills TJ, Paschke SS, Keith G, Linard JI (2014) Mobilization of selenium from the Mancos Shale and associated soils in the lower Uncompahgre River Basin, Colorado. App Geochem 48:16–27

McNeal JM, Balistrieri LS (1989) Selenium in agriculture and the environment: geochemistry and occurrence of selenium an overview.

American Society of America and American Society of Agronomy, pp 1–13
Morrison SJ, Spangler RR (1992) Extraction of uranium and molybdenum from aqueous solutions: a survey of industrial materials for use in chemical barriers for uranium mill tailings remediation. Environ Sci Technol 26:1922–1931
Mount Sopris Instruments (2017) https://mountsopris.com/. Accessed 22 Feb 2018
Naftz DL, Rice JA (1989) Geochemical processes controlling selenium in ground water after mining, Powder River Basin, Wyoming, USA. App Geoch 4:565–575
National Uranium Resource Evaluation (NURE) (2017) Hydrogeochemical and stream sediment reconnaissance data. NURE. https://mrdata.usgs.gov/metadata/nurehssr.faq.html. Accessed 1 May 2017
New Mexico Bureau of Geology and Mineral Resources [NMBGMR] (2003) Geologic map of New Mexico, scale 1:500,000. https://geoinfo.nmt.edu/publications/maps/geologic/state/home.cfml. Accessed 1 May 2017
New Mexico Environment Department (NMED) (2008) Preliminary assessment report: San Mateo Creek legacy uranium sites. https://www.epa.gov/sites/production/files/2015-06/documents/06-93397 67.pdf. Accessed 1 May 2017
New Mexico Environment Department (NMED) (2012) Site inspection report, Phase 2, San Mateo Creek Basin legacy uranium mine and mill site area, CERCLIS ID NMN000606847, Cibola-McKinley Counties, New Mexico. https://www.epa.gov/sites/production/files/2015-05/documents/san_mateo_creek_si_phase_2-report_final.pdf. Accessed 1 May 2017
Schoeppner J (2008) Groundwater remediation from uranium mining in New Mexico. Southwest Hydrol 7:22–23
Turner-Peterson CE, Fishman ES (1986) Fluvial sedimentology of a major uranium-bearing sandstone—a study of the Westwater Canyon Member of the Morrison Formation, San Juan basin, New Mexico. In: Turner-Peterson CE, Santos ES, Fishman NS (eds) A Basin Analysis Case Study: The Morrison Formation, Grants Uranium Region, New Mexico, vol 22. American Association of Petroleum Geologists Studies in Geology, pp 47–75
United States Environmental Protection Agency (EPA) (2010) Focused Review of Specific Remediation Issues, Report F, An Addendum to the Remediation System Evaluation for the Homestake Mining Company (Grants) Superfund Site, New Mexico. Prepared by US Army Corps of Engineers Environmental and Munitions Center of Expertise for US Environmental Protection Agency, Region, vol 6, p 428
United States Environmental Protection Agency (EPA) (2011) Third Five-Year Review Report, Homestake Mining Company Superfund Site, Cibola County, Region 6. United States Environmental Protection Agency, Dallas, p 133
United States Environmental Protection Agency (EPA) (2016) Drinking water requirements for states and public water systems, Radionuclides rule. https://www.epa.gov/dwreginfo/radionuclides-rule#rule-summary. Accessed 22 Feb 2018
United States Environmental Protection Agency (EPA) (2018) Phase 2 Ground-Water Investigations Report for the San Mateo Creek Basin Legacy Uranium Mines Site, Cibola and McKinley Counties, Region 6. United States Environmental Protection Agency, Dallas, p 244
United States Geological Survey (USGS) (variously dated), National field manual for the collection of water-quality data, techniques and method book 9, accessed April 4, 2018, at https://water.usgs.gov/owq/FieldManual/index.html
Van Berk W, Fu Y (2017) Redox roll-front mobilization of geogenic uranium by nitrate input in aquifers: risks for groundwater resources. Environ Sci Technol 51:337–345. https://doi.org/10.1021/acs.est.6b01569
Vroblesky DA, Petkewich M, Campbell T (2002) Field tests of diffusion samplers for inorganic constituents in wells and at a ground water discharge zone. U.S. Geological Survey Water-Resources Investigations Report 02-4031, p 31
Vroblesky DA, Manish J, Morrell J, Peterson JE (2003a) Evaluation of passive diffusion bag samplers, dialysis samplers, and nylon-screen samplers in selected wells at Andersen Air Force Base, Guam, March-April 2002. U.S. Geological Survey Water-Resources Investigations Report 03-4157, p 36
Vroblesky D, Scheible W, Teall G (2003b) Laboratory Equilibration Study of Nylon-Screen Passive Diffusion Samplers for VOCs, and Select Inorganics. Presented at ITRC Spring Meeting, March 2003, Annapolis MD
Wright GW (1999) Oxidation and mobilization of selenium by nitrate in irrigation drainage. J Environ Qual 28(4):1182–1187. https://doi.org/10.2134/jeq1999.00472425002800040019x
Zielinski RA, Chafin DT, Banta ER, Szabo BJ (1997) Use of ^{234}U and ^{238}U isotopes to evaluate contamination of near-surface groundwater with uranium-mill effluent: a case study in south-central Colorado. USA Environ Geol 32(2):124–136